Supporting Information

Electrochemical Conversion of KA Oil by Indium Tin Oxide Nanospheres and Nanocubes

Yanwei Li[a, b], Longbin Liu[c], Lu Qiu[c], Jia Huang[d], Yi Shen[a, b, *]

[a] School of Food Science and Engineering, South China University of Technology, Guangzhou, 510640, China

[b] China-Singapore International Joint Research Institute, Guangzhou Knowledge City, Guangzhou, 510663, China

[c] School of Energy and Power Engineering, Beihang University, Beijing, 100191, China

[d] Research Institute of Aerospace Technology, Central South University, Changsha, 410083, China

[*]Corresponding author, Email: feyshen@scut.edu.cn

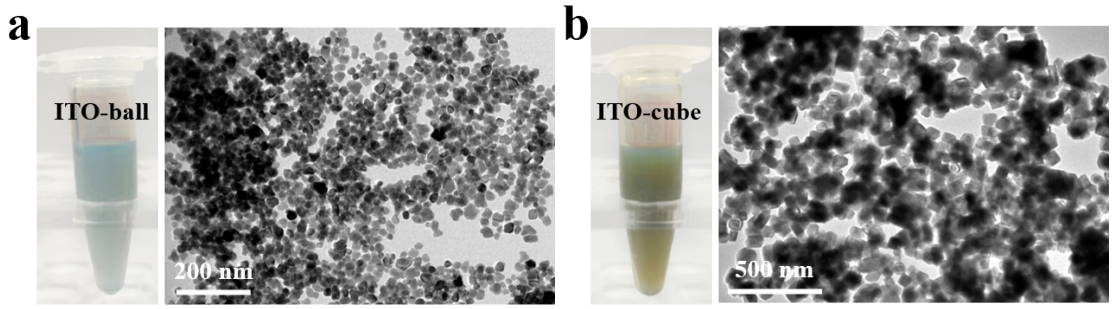

Fig. S1 Digital pictures and TEM images of (a) ITO-ball and (b) ITO-cube.

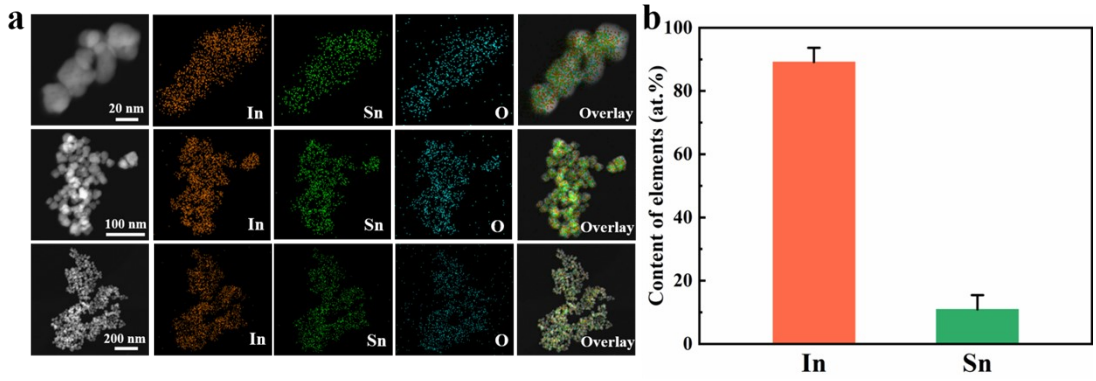

Fig. S2 (a) TEM-EDX elemental mapping images of In, Sn and O for the ITO-ball samples, and (b) the corresponding content of elements obtained by EDX.

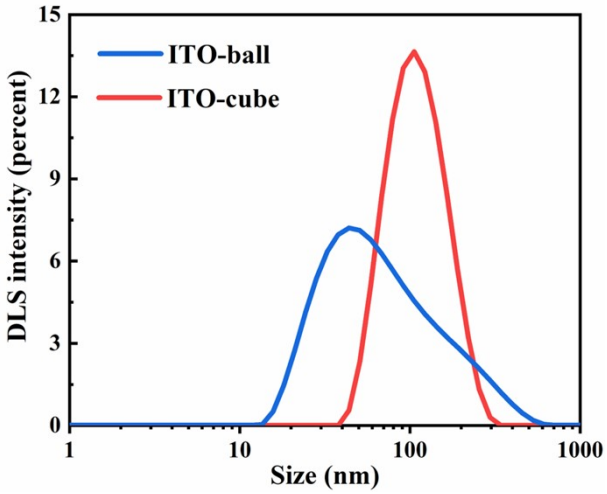

Fig. S3 Hydrodynamic size distribution of the samples.

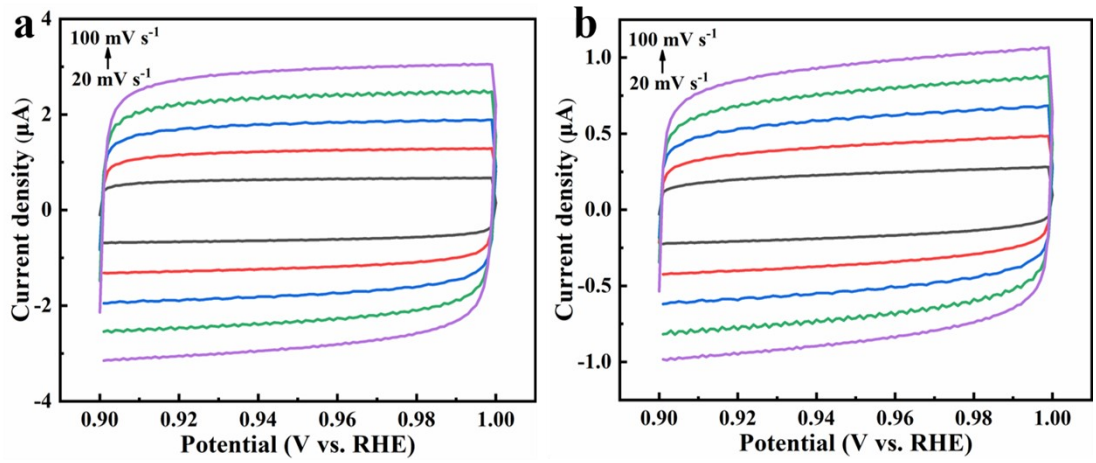

Fig. S4 CV curves of (a) ITO-ball and (b) ITO-cube recorded at different scan rates within the non-Faradic region in 1 M KOH solutions.

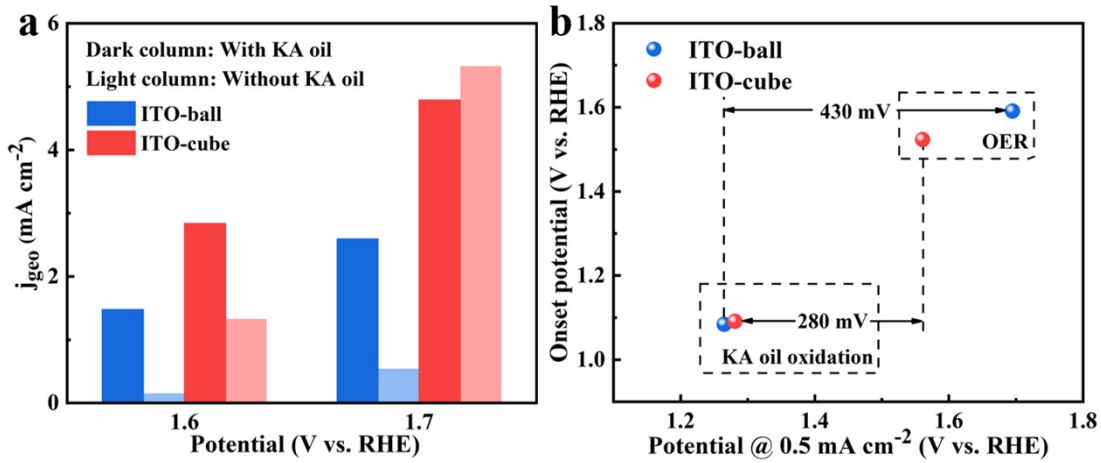

Fig. S5 (a) Current densities of OER and KA oil oxidation over the two samples at 1.6 and 1.7 V, and (b) comparison of the two samples towards OER and KA oil oxidation based on the *ECSA*-normalized LSV curves.

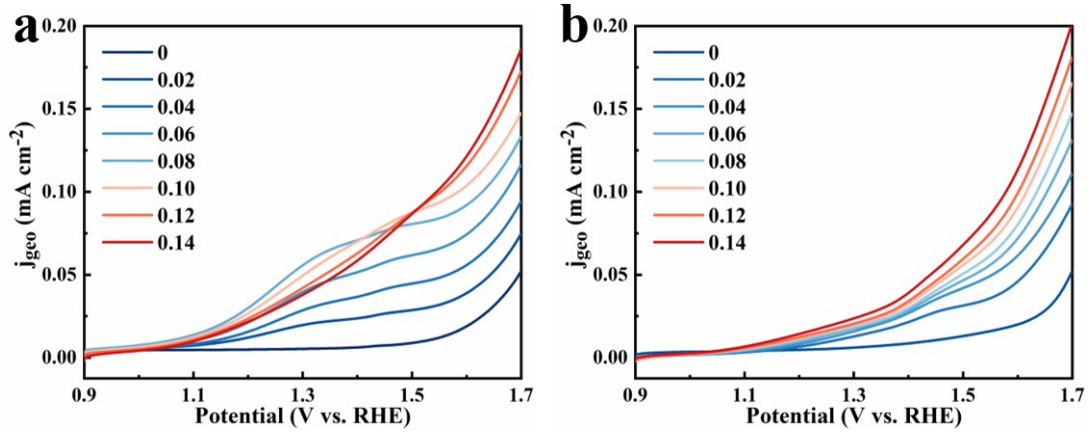

Fig. S6 LSV curves of (a) ITO-ball and (b) ITO-cube recorded with varied $C_{KA\ oil}$ (0 - 0.14 M) and fixed C_{OH^-} (1 M).

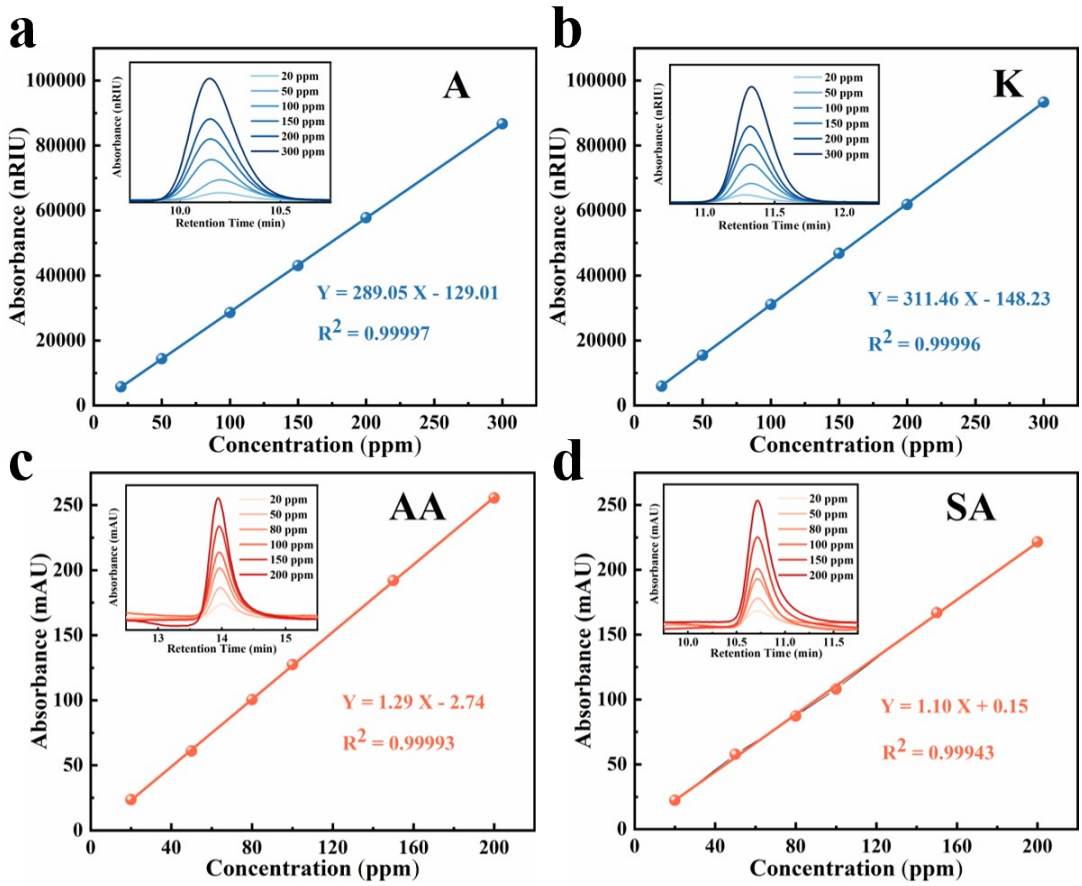

Fig. S7 Standard HPLC curves of (a) cyclohexanone, (b) cyclohexanol, (c) adipic acid, and (e) succinic acid.

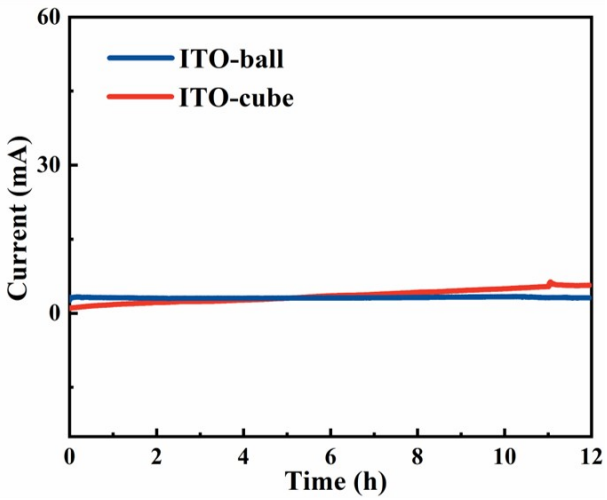

Fig. S8 I-t curves of KA oil electro-oxidation over ITO-ball and ITO-cube at 1.6 V vs. RHE in 1 M KOH with 0.5 M KA oil for 12 hours.

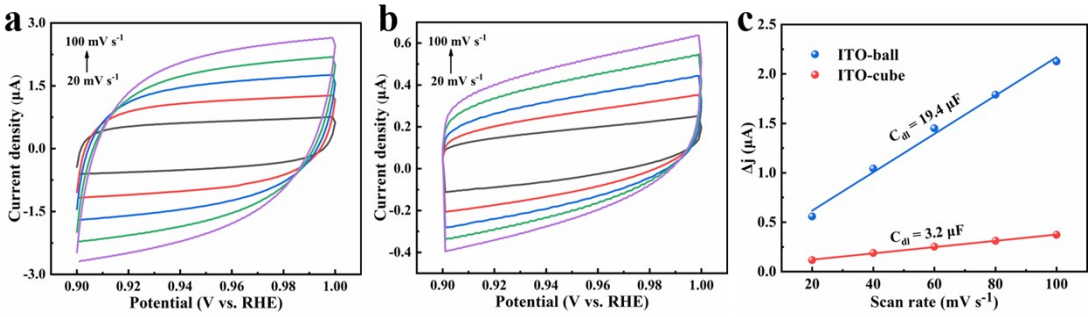

Fig. S9 CV curves of (a) ITO-ball and (b) ITO-cube recorded at different scan rates within the non-Faradic region in 1 M KOH + 0.1 M KA oil solutions, and (c) corresponding current difference $(i_a\text{-}i_c)/2$ plotted against scan rate.

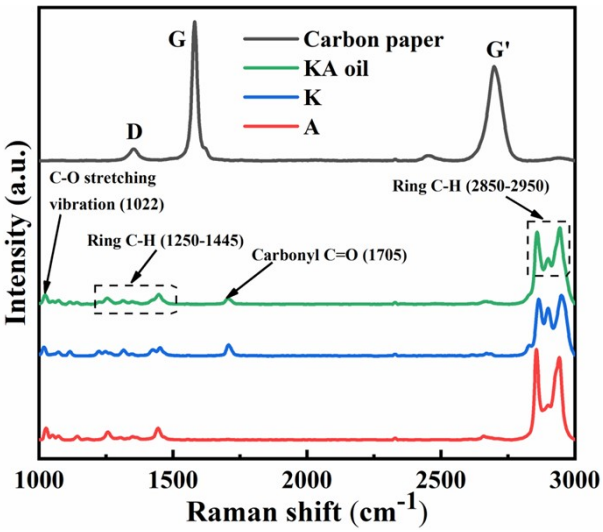

Fig. S10 Raman spectra of carbon paper, K, A, and KA oil solutions.

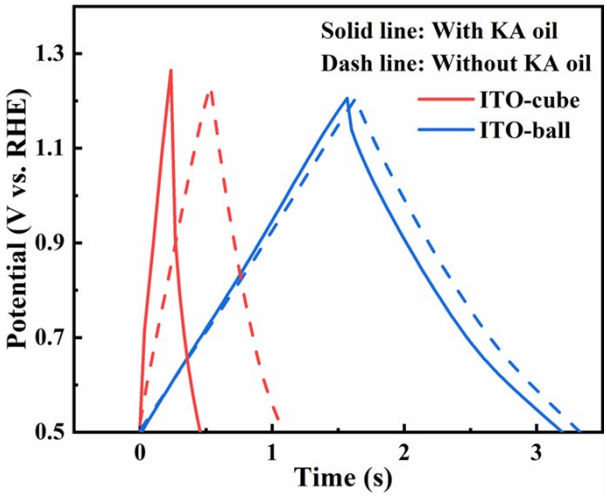

Fig. S11 Galvanostatic charge-discharge (GCD) curves of ITO-ball and ITO-cube in 1 M KOH with or without KA oil at 0.2 mA cm^{-2}.

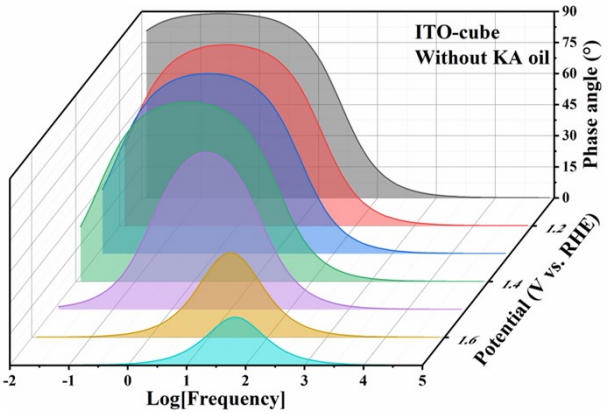

Fig. S12 Bode phase plots of ITO-cube recorded in 1 M KOH solutions at different potentials.

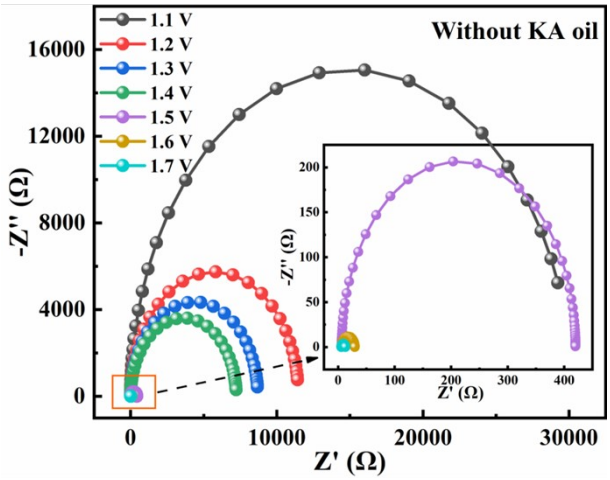

Fig. S13 Nyquist plots of ITO-cube recorded in 1 M KOH solutions at different potentials.